

Two-stream Model of the Pulsed Plasma Thruster and Simulation Research

IEPC-2017-321

*Presented at the 35th International Electric Propulsion Conference
Georgia Institute of Technology • Atlanta, Georgia • USA
October 8 – 12, 2017*

Xiaoyan Cheng¹, Xiangyang Liu², Zhiwen Wu, Kan Xie, Ningfei Wang
Beijing Institute of Technology, Beijing, 100081, China

Xuning Zhang
Jiangmen Polytechnic, Jiangmen Guangdong, 529090, China

Abstract: Pulsed plasma thruster (PPT) is a promising electric propulsion device with high specific impulse and light weight. Researchers have conducted various simulation and experimental research for years to help understand the working principle of PPT. Yet current slug models could not completely simulate emission process inside the electrode channel of an APPT. According to high-speed photography, there are two plasma streams flowing downstream during the discharge. This paper proposes a two-stream model based on the earlier slug model which regards the plasma in APPT as two plasma streams that appear in the discharge region successively. The numerical results show that the discharge and motion processes are in good agreement with experimental results of high-speed photography. Compare two-stream model with slug model, the two-stream model has more reasonable simulation results according to experiments. The numerical results also show that nearly 75% of the impulse bit and 70% of the charged mass are consumed in the first plasma stream.

Nomenclature

| | |
|------------|---------------------------|
| B | = magnetic flux density |
| C | = capacitance |
| R | = resistance |
| L | = inductance |
| V_0 | = initial voltage |
| μ_0 | = permeability of vacuum |
| h | = electrode gap |
| w | = electrode width |
| V_{cirt} | = Alfvén critical speed |
| m_p | = charged mass of plasma |
| F_{gas} | = aerodynamic force |
| k | = Boltzmann constant |
| n | = particle number density |
| T_p | = plasma temperature |
| J | = current density |

¹ Master student, School of Aerospace Engineering, 2120160048@bit.edu.cn

² Associate Professor, School of Aerospace Engineering, liuxy@bit.edu.cn, the corresponding author.

I. Introduction

Pulsed Plasma Thruster has been a research focus for its potential application for micro-satellite such as Cubсата¹. Over the past 50 years, there has developed various prototype PPTs with different structure. The theoretical research on the working process of PPT is also synchronized to meet the requirements of complex space mission².

The schematic of a parallel-plate PPT is shown in Fig.1. A solid propellant bar, usually Teflon, fills the gap between two electrodes connected to a charged capacitor in vacuum. Once the ignition signal is sent, the spark plug starts to work and produces the initial plasma, triggering an electrical arc across the exposed surface of the Teflon, which is then accelerated by electromagnetic and pressure forces³.

In order to study the work process of PPT, researchers have built a number of mathematical models together with advanced testing methods, to simulate and measure performance parameters of the thruster. In 1968, Jahn put forward a slug model to describe the PPT system as an electromechanical device that interacts with kinetic system, which lay a theoretical foundation for the follow-up study⁴. L.Yang et al. developed a new method to evaluate the influence of gas-dynamic effect on the thrust and ablation performance of PPT⁵. G.A.Popov et al. developed a new physic-mathematical model of plasma acceleration to simulate the low thrust APPT in RIAME⁶. But the slug model has some disadvantages. The model consider there is only one plasma stream between the electrodes gap being accelerated during one shot⁷, which is not consistent with the experimental results. Also it could not explain the phenomenon that the discharge is still going on when plasma stream flow out of electrodes.

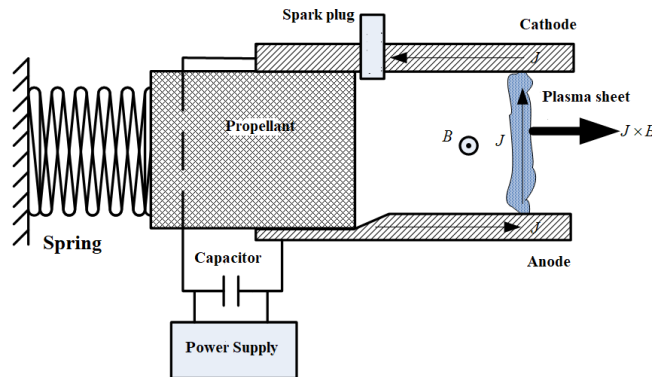


Figure 1. Schematic of a PPT.

According to Hiroyuki Koizumi and Ryosuke Noji's research⁸, there are two plasma streams flowing downstream successively and the neutral particles remain near the propellant surface as can be seen from Fig 2 and Fig 3. Figure 2 shows images of 426nm emission line from ions C⁺ which is the main component of plasma sheet⁹.

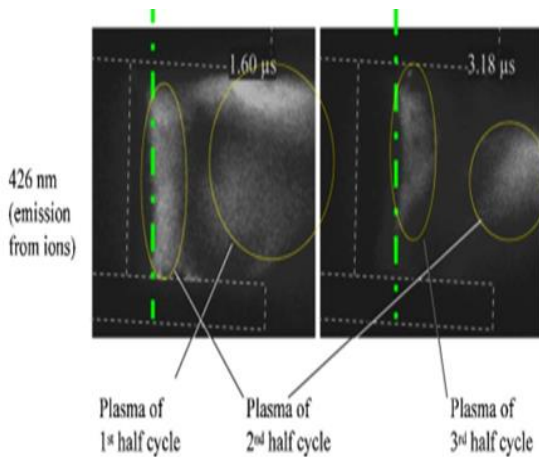


Figure 2. The successive images of plasma streams

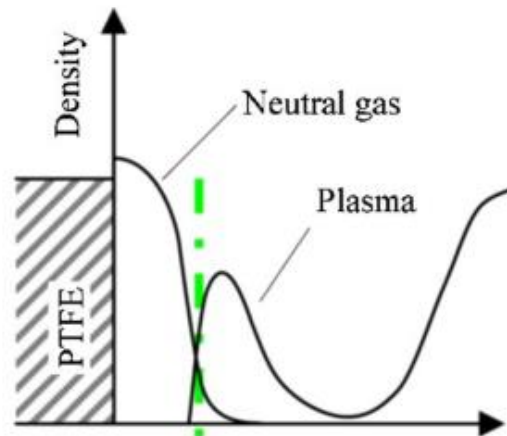


Figure 3. The density of plasma and neutral gas

To simulate the evolution of plasma streams between the electrodes gap, Tiankun Huang built a developed slug model which is based on the assumption that plasma flow is discontinuous with a number of plasma streams¹⁰. But the simulation results in Huang's paper don't include the motion of multiple plasma streams and for convenience, the motion model in Huang's paper considers that two plasma streams collide fuse together form a single plasma stream.

In order to simulate the motion of plasma streams more accurate, a two-stream model based on electromechanical model is established in this paper. The model contains circuit model, magnetic field model, movement model etc. The motion processes of plasma and charged currents in two APPTs are simulated to validate the new model.

II. Theoretical modeling

A. Assumption

Assumption I: based on motion of plasma streams observed by high-speed photography, it is assumed that there are three periodic processes of the discharge during one shot before modeling as Fig. 4 shows:

- 1) $0 < t < t_1$, it has one major plasma stream and an initial weak plasma stream near the propellant surface¹¹, neutral gas produce and convert to plasma.
- 2) $t_1 < t < t_2$, one plasma stream flow downstream and neutral gas gather near the propellant with weak plasma.
- 3) $t_2 < t < t_4$, there exist two plasma streams since the neutral gas gathered last process start to convert to plasma. The third stream appears when $t=t_4$ roughly.

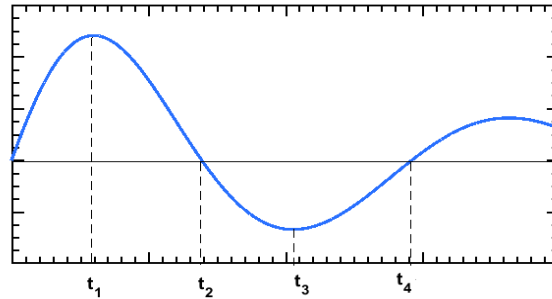


Figure 4. Three processes of the discharge.

Assumption II: the resistance of each plasma stream is constant during the discharge;

Assumption III: the electrodes thickness is negligible and the current on the plasma streams are uniform.

Assumption IV: the plasma stream disappear and do not contribute to movements if it leaves the end of electrodes.

B. Circuit Model

The discharge circuit of PPT are made up of resistance and inductance of the capacitor, wires and plasma streams. As shown in Fig. 5, it can be described as LRC circuit with two plasma branches according to two-stream model. Herein, R_1 , L_1 are the resistance and inductance of the first plasma stream respectively. R_2 , L_2 are those of the second plasma stream. R_e is the resistance of transmission line and R_c is the resistance of capacitor. L_e and L_c are the inductance of transmission line and capacitor respectively. I_1 and I_2 are the current of plasma streams.

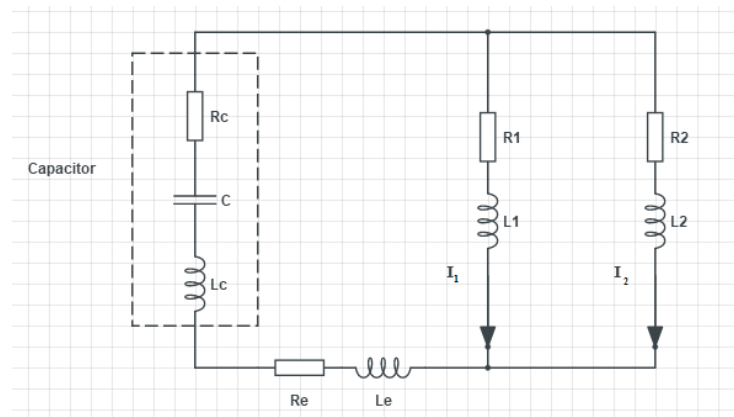


Figure 5. LRC circuit model.

According to Kirchoff's law, the equation of the equivalent circuit can be computed as:

$$\begin{cases} C \frac{du_c}{dt} + I_1 + I_2 = 0 \\ L_1 \frac{dI_1}{dt} + I_1 R_1 = u_c = L_2 \frac{dI_2}{dt} + I_2 R_2 \\ u_c = u_0 - \frac{1}{C} \int_0^t I_{tot}(t) dt = R_T I_{tot} + \frac{d}{dt} [L_T(t) I_{tot}] \end{cases} \quad (1)$$

Where C and u_c are the capacitance and voltage of capacitor and u_0 is the initial voltage. $I_{tot}(t)$ is the discharge current of capacitor, R_T and $L_T(t)$ are the total resistance and inductance of the RLC circuit.

C. Magnetic Field Model

During the process of two streams, the magnetic field distribution between electrodes is described as separate rectangular solenoid as shown in Fig.6. I_1 , I_2 are currents on each plasma stream. In this paper, the electrodes thickness is negligible and the current on the plasma streams are uniform according to assumption III¹².

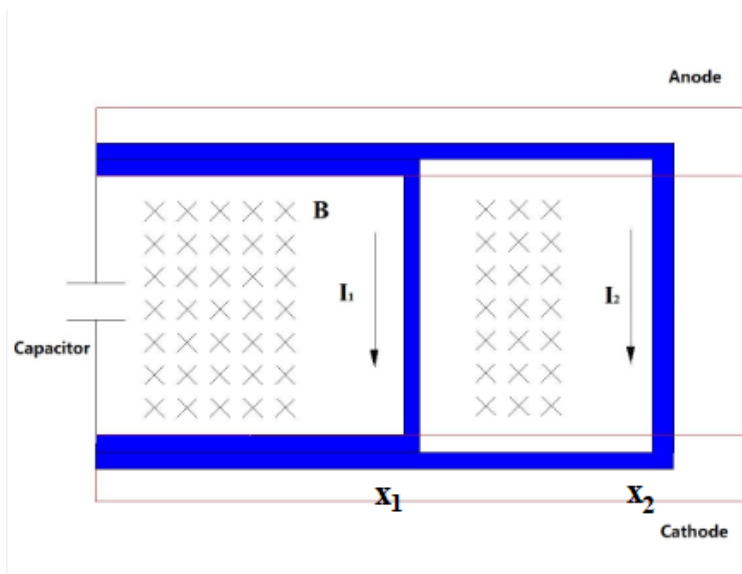


Figure 6. Schematic of the magnetic field model.

For previous slug model, the magnetic field is shown as follows:

$$B(x,t) = \begin{cases} \mu_0 \frac{I(t)}{w}, 0 < x \leq x(t) \\ 0, x > x(t) \end{cases} \quad (2)$$

Where $B(x,t)$ is the intensity of magnetic field at position x and time t , μ_0 is the permeability of vacuum and $x(t)$ is the position of the plasma stream, start from the surface of propellant.

For two-stream model, the total intensity of magnetic field can be superimposed as:

$$B(x,t) = \begin{cases} \mu_0 \frac{I_1}{w} + \mu_0 \frac{I_2}{w}, & x < x_1(t) \\ \mu_0 \frac{I_2}{w}, & x_1(t) < x < x_2(t) \\ 0, & x > x_2(t) \end{cases} \quad (3)$$

Where x_1, x_2 are the distance between plasma stream and the surface of propellant. The distribution of the inductance between electrodes can be computed by integration of magnetic field.

D. Motion Model

Each plasma stream is accelerated by the Lorentz force and aerodynamic force. In addition, the plasma stream disappear and do not contribute to movements if it leaves the end of electrodes. According to Newton's second law and assumption IV, the motion equation of each plasma stream is:

$$\frac{d}{dt}[m\dot{x}(t)] = \iiint J(t) \times B(x,t) dV + F_{gas} \quad (4)$$

Where m is the mass of each plasma stream and $J(t)$ is current density. F_{gas} refers to aerodynamic force which is significantly less than the Lorentz force¹³. Therefore F_{gas} is computed as constant in this paper.

$$F_{gas} = hwnkT_p \quad (5)$$

Herein, k is Boltzmann constant and has a value of 1.38×10^{-23} J/K, n is particle number density and T_p is plasma temperature.

E. Ablation Model

It is generally considered with the experiment conclusion that the ablation mass is linear with the discharge energy. To facilitate the calculation of plasma mass, the flow of plasma is described as an idealized, quasi-steady flow¹⁴. There exists a magneto-sonic point at some position along the discharge channel in the magneto-hydrodynamic flow with a high magnetic Reynolds number and magnetic pressure much greater than the plasma pressure. The conditions at this point are then used to scale the exhaust velocity by the Alfvén critical speed and estimate the plasma mass flow rate at the surface of the propellant.

$$\dot{m}_p = \frac{A\mu_0 I^2}{4.404w^2V_{crit}} \quad (6)$$

Where A is the ablation area and the product of h and w . V_{crit} is the Alfvén critical speed and have a value of 1.3×10^4 m/s for PTFE.

By integrating Eq. 6, it could be gained as

$$m_p(t) = \frac{\mu_0 h}{4.404wV_{crit}} \int_0^t I_i^2(t) dt \quad (7)$$

Where I_i is the current of each plasma stream.

F. Integrated Equations and Programming

Combined the above equations (1), (3), (4), (6), (7) with the equations of LRC electric circuit and Newton mass motion. The two-stream model based on electromechanical model can be evolved to simulate the discharge process of APPT. It is an ordinary differential equations and be numerically solved by the Runge-Kutta algorithm.

III. Model Verification and Discussion

A. Model Verification and Simulation Result

The discharge process of the APPT used in University of Tokyo is simulated in this paper. For convenience, the APPT used in U-Tokyo is simply called APPT I in this paper. The operation parameters of APPT I are provided in Table 1.

The simulated waveforms of current using two-stream model are shown in Fig. 8 with initial operation parameters of the APPT I. The current waveforms obtained from experimental measurement is shown in Fig. 7. As can be seen in Fig. 8, I_1 is current of the first plasma stream and I_2 is the second one, I_3 is current of the third weak plasma stream. I_t is the total current of circuit loop which has good agreement with the experimental data. According to assumption I that at the beginning of the discharge, there has initial weak plasma near the propellant surface so that it exists two current waveforms during the whole discharge process.

Table 1. The operation parameters of APPT I

| Operation Parameter | Value |
|---|-------|
| Electrode Width (mm) | 10 |
| Electrode Length (mm) | 25 |
| Electrode Gap (mm) | 20 |
| Voltage (V) | 2200 |
| Capacitor (μF) | 3.0 |
| Initial resistance ($\text{m}\Omega$) | 48 |
| Initial inductance (nH) | 80 |

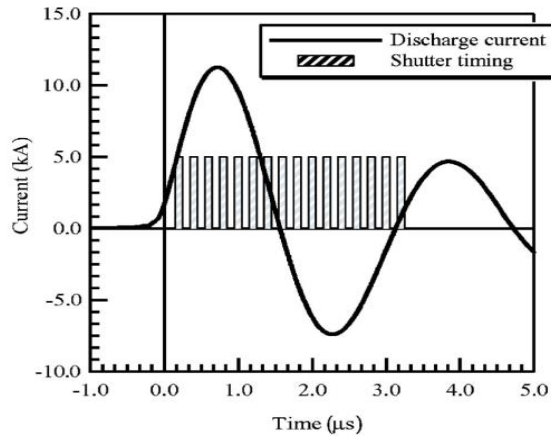


Figure 7. Discharge current of the APPT I

The simulated displacement curve of APPT I is shown in Fig. 9 and the successive images of plasma streams are shown in Fig. 2. As can be seen from the simulation results, when time t comes to t_2 , also $t \approx 1.4 \mu\text{s}$ in Fig. 9, the second plasma stream begins to accelerate. According to high-speed photographic images, there is an initial displacement when the second plasma stream emerge because the neutral gas sheet slowly moves downstream and during the time a part of neutral gas convert to plasma. When time comes to t_3 (roughly $2.2 \mu\text{s}$ in Fig. 9), the first plasma stream flow out of electrodes. The displacement curve is in good agreement with the motion of the plasma stream in high-speed photography.

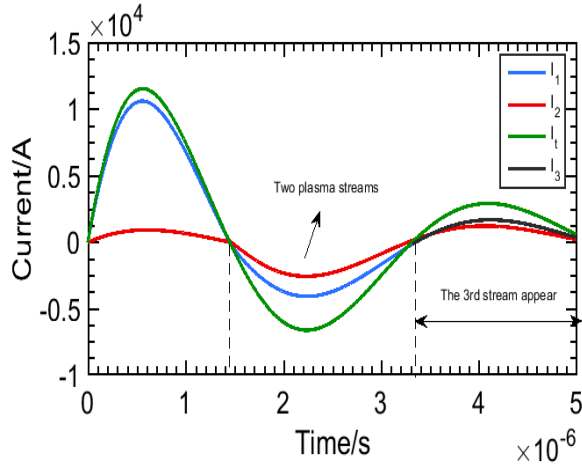


Figure 8. Simulated current of the APPT I

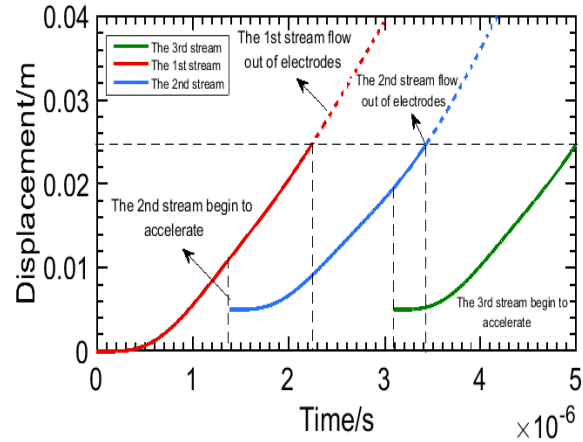


Figure 9. Simulated displacement of the APPT I

The simulated velocity of two plasma streams are shown in Fig. 10. As can be seen from it, when time comes to $1.4\mu\text{s}$ roughly, the second plasma stream begins to accelerate and the first stream's growth of velocity slows down. The exit velocity of the first plasma stream is about 18 km/s and the second one is about 17 km/s . The steady velocity of the third plasma stream is about 14 km/s . The ion exhaust velocity was calculated as $10\text{--}20\text{ km/s}$ from the images and according to the Alfvén critical velocity, singly ionized carbon is calculated as 13 km/s ¹⁵, which all fit well with the simulated velocity. And the simulation results also show that the exit velocity of each plasma stream are roughly equal.

The ablation mass of plasma simulated by two-stream model is shown in Fig. 11. It can be judged that ratio of the three plasma's ablation mass is about $2.3:0.9:0.18$, which means most of the ablation mass (94%) was consumed in the first two plasma streams.

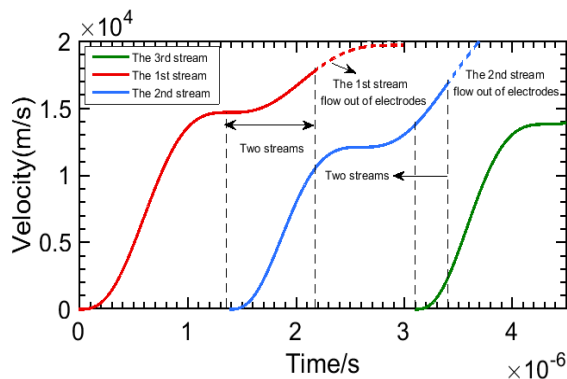


Figure 10. Simulated velocity of the APPT I

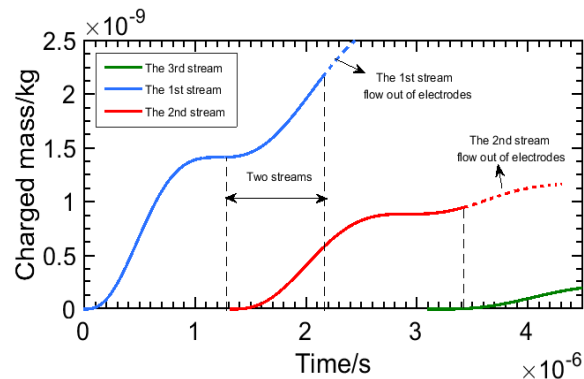


Figure 11. Simulated charged mass of the APPT I

To test the applicability of two-stream model and accuracy of performance parameter simulation like impulse bit, specific impulse etc, the discharge process of an APPT used in Beijing Institute of Technology called APPT II in this paper is also simulated. The operation parameters of APPT II are shown in Table 2.

Table 2. The operation parameters of APPT II

| Operation Parameter | Value |
|---|-------|
| Electrode Width (mm) | 12 |
| Electrode Length (mm) | 17 |
| Electrode Gap (mm) | 25 |
| Voltage (V) | 1500 |
| Capacitor (μF) | 2.0 |
| Initial resistance ($\text{m}\Omega$) | 40 |
| Initial inductance (nH) | 65 |

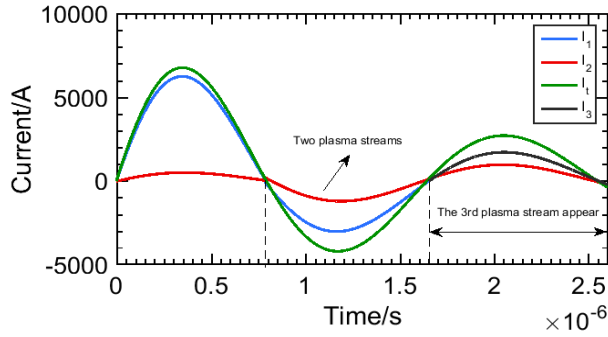


Figure 12. Simulated and experimental current of APPT II

The current waveforms obtained from experiments and simulations are shown in Fig 12. The simulation results are also close to the experimental results. The displacement and velocity curves obtained from simulation results are shown in Fig 13, Fig 14 respectively. As can be seen from these figures, the first stream flow out of electrodes when time gets to $2.5\mu\text{s}$ with the exit velocity of 9.5 km/s . The distance between the 2nd and 3rd stream are about 3mm so there is no clear boundary between the these two streams considering the thickness of them. The velocity of the 2nd and 3rd streams are about 5 km/s much lower than the first one, which is different from the simulation results of APPT I. Further research will focus on the influence of different operation parameters on the motion of two or more plasma streams.

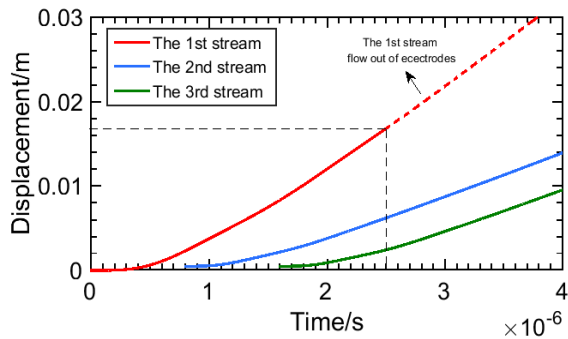


Figure 13. Simulated displacement of the APPT II

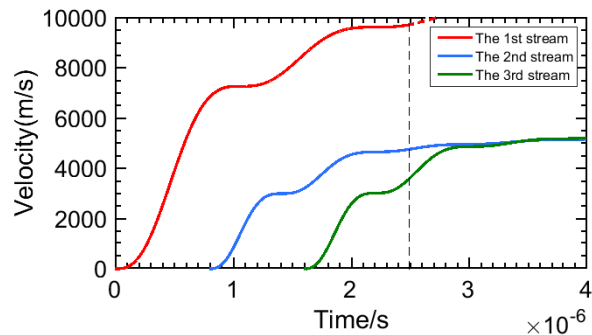


Figure 14. Simulated velocity of the APPT II

The performance parameters obtained from the simulation results of APPT II are shown in Table 3. It can be concluded that the 1st stream contributes 75% of the impulse bit and 70% of the charged mass. In general, the simulation performance parameters are in good agreement with the experimental results.

Table 3. The simulation and experimental results of performance parameters

| Performance parameters | Simulation | | | | Experiment |
|---|----------------------------|----------------------------|----------------------------|-------|------------|
| | The 1 st stream | The 2 nd stream | The 3 rd stream | Total | |
| Impulse bit/ $\mu\text{N}\cdot\text{s}$ | 32 | 9 | 2 | 43 | 51 |
| Charged mass/ μg | 0.5 | 0.16 | 0.03 | 0.7 | none |
| Total ablated mass/ μg | | 5.9 | | | 6.3 |
| Efficiency/% | | 11.8 | | | 12.2 |
| Specific impulse/s | | 744 | | | 874 |

B. Comparison of Simulated Results between the Slug and Two-stream Models

The simulation results of the slug model and two-stream model based on APPT I are compared in this section. The comparison of the simulated current is shown in Fig. 15. Table 4 lists some characteristic current points of two simulation methods and the experimental current data for the purposes of comparison. As can be seen from them, the two current curves are in good agreement before time t_2 and after that, the current simulated by two-stream model is closer to the experimental current data.

Table 4. The comparison of current simulated by two models

| Slug model | | Two-stream model | | The experimental current | |
|---------------|------------|------------------|------------|--------------------------|------------|
| Time/ μ s | Current/kA | Time/ μ s | Current/kA | Time/ μ s | Current/kA |
| 0.62 | 12.1 | 0.56 | 12.1 | 0.7 | 11.8 |
| 1.39 | 0 | 1.37 | 0 | 1.56 | 0 |
| 2.1 | -6.7 | 2.20 | -8.3 | 2.28 | -7.9 |
| 2.93 | 0 | 3.16 | 0 | 3.12 | 0 |
| 3.62 | 4.1 | 3.96 | 4.9 | 3.9 | 4.7 |

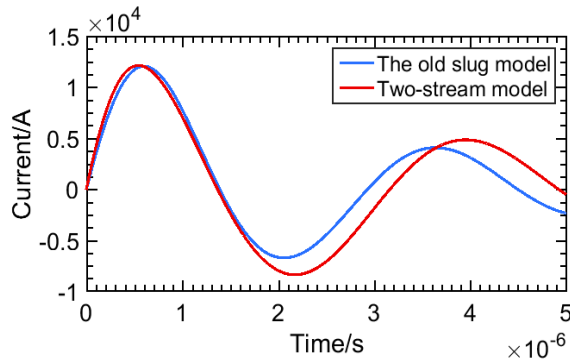


Figure 15. The comparison of simulated current

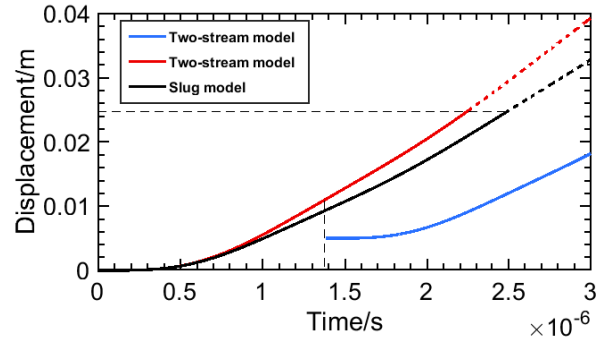


Figure 16. The comparison of simulated displacement

The comparison of simulated displacement, velocity and charged mass between the slug and two-stream model are shown in Fig. 16, 17 and Fig. 18 respectively. It can be seen from them that the displacement and velocity simulated by slug model are less than the first stream's simulation results and the charged mass are larger. Because the old slug model considers all charged gas as one plasma stream which is not consistent with the experimental observations, the simulated results by two-stream model are more reasonable and more closer to experimental results.

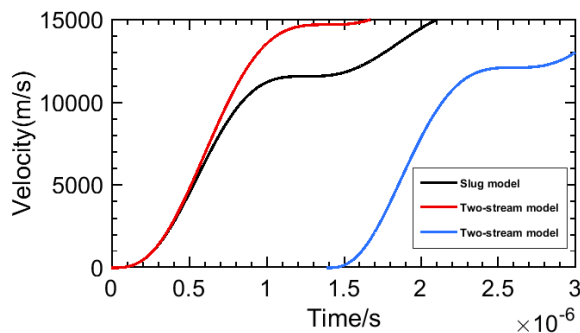


Figure 17. The comparison of simulated velocity

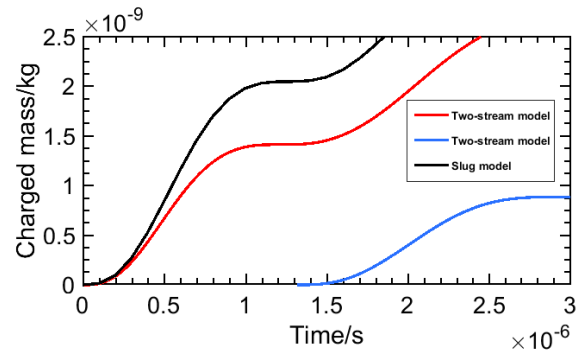


Figure 18. The comparison of simulated charged mass

IV. Conclusion

A two-stream electromechanical model based on the slug model has been established in this paper. The discharge process and plasma flow process have been simulated by two-stream model. The conclusions are as follows.

- (1) According to the experimental results, the two-stream model has better simulated current curve and more reasonable motion process of plasma streams compared with the slug model. And the displacement and velocity simulated by slug model are less than the first stream's simulation results but the charged mass are larger.
- (2) The simulated current of APPT I and II are similar to the experimental data in the matter of peak current and current phase. The simulated motion of APPT I like displacement, velocity are in good agreement with the results of high-speed photography. The simulated performance parameters of APPT II like impulse bit, efficiency are also similar to the experimental results.
- (3) 69% of the charged plasma mass was consumed in the first plasma stream and 27% the second one according to simulation results of APPT I. The first stream contributes 75% of the impulse bit and 70% of the charged mass according to simulation results of APPT II.

Acknowledgments

This research was supported by Chinese National Natural Science Foundation (51576018).

References

- ¹ A. Mingo Pérez, M. Coletti, and S. B. Gabriel, "Development of a microthruster module for nanosatellite applications, " in Proc. 32nd Int. Electr. Propuls. Conf., Wiesbaden, Germany, 2011.
- ² Matthias Lau, Georg Herdrich, "Pulsed plasma thruster – subsystem engineering at IRS", in: Proceedings of the 34th International Electric Propulsion Conference, IEPC-2015-21, Hyogo, Kobe, Japan, 2015.
- ³ R. L. Burton, P. J. Turchi. "Pulsed Plasma Thruster." Journal of Propulsion and Power. Vol. 14, No. 5, September – October 1998
- ⁴ Jahn, Robert G, and F. A. Lyman. "Physics of Electric Propulsion. McGraw-Hill", 1968.
- ⁵ Yang, L., Liu, X. Y., Wu, Z. W. & Wang, N. F. (2011). "Analysis of Teflon Pulsed Plasma Thrusters Using a Modified Slug Parallel Plate Model". In 47th AIAA/ASME/SAE/ASEE Joint Propulsion Conference & Exhibit, San Diego, USA.
- ⁶ Popov, G. A., et al. "Physicomathematical model of plasma acceleration in an ablative pulsed plasma thruster." Plasma Physics Reports 40.5(2014):336-342.
- ⁷ Cassibry, J. T., et al. "Numerical Modeling of a Pulsed Electromagnetic Plasma Thruster Experiment." Journal of Propulsion & Power 22.3(2015):628-636.
- ⁸ Koizumi, Hiroyuki, et al. "Plasma acceleration processes in an ablative pulsed plasma thruster." Physics of Plasmas 14.3(2007):716.
- ⁹ Koizumi, Hiroyuki, et al. "Study on Plasma Acceleration in an Ablative Pulsed Plasma Thruster." Physics of Plasmas 14.3(2007):033506-033506-10.
- ¹⁰ Huang, Tiankun, et al. "Modeling of gas ionization and plasma flow in ablative pulsed plasma thrusters." Acta Astronautica 129(2016):309-315.
- ¹¹ AIAA. "Energy balance and efficiency of the pulsed plasma thruster." *Aiaa/asme/sae/asee Joint Propulsion Conference and Exhibit* 1998:434-44.
- ¹² David Daniel Laperriere. "Electromechanical Modeling and Open-Loop Control of Parallel-Plate Pulsed Plasma Microthrusters with Applied Magnetic Fields". M.S.Thesis, Worcester Polytechnic Institute, 2005.
- ¹³ Solbes, A., K. Thomassen, and R. Vondra. "Analysis of solid Teflon pulsed plasma thruster." Journal of Spacecraft & Rockets 7.7(2013):1402-1406.
- ¹⁴ Turchi, P.J., Mikellides, I.G., Mikellides, P.G. & Kamhawi, H. (1999). " Optimization of Pulsed Plasma Thrusters for Microsatellite Propulsion". In 35th AIAA/ASME/SAE/ASEE Joint Propulsion Conference and Exhibit, Los Angeles, USA.
- ¹⁵ R. L. Burton, F. Rysanek, E. A. Antonsen, M. J. Wilson, and S. S. Bushman, in *Micropropulsion for Small Spacecraft*, edited by M. M. Micci and A. D. Ketsdever (American Institute of Aeronautics and Astronautics, Washington, D.C., 2000), Chap. 13.